Regio- and prenylation mode specificities of the fungal indole diterpene prenyltransferases, AtmD and PaxD

Chengwei Liu,[a] Atsushi Minami,[b] Motoyoshi Noike,[a] Hiroaki Toshima,[c] Hideaki Oikawa,[b] and Tohru Dairi[a]*

Graduate School of Engineering, Hokkaido University, Sapporo, Hokkaido 060-8628, Japan[a]; Graduate School of Science, Hokkaido University, Sapporo, Hokkaido 060-0810, Japan[b]; College of Agriculture, Ibaraki University, Inashiki, Ibaraki 300-0393, Japan[c]

Running Head: Prenyltransferases with broad substrate specificity

*Corresponding author
E-mail: dairi@eng.hokudai.ac.jp
Tel: +81-11-706-7815
Fax: +81-11-706-7118

Abstract We recently reported the function of *paxD*, which is involved in the paxilline (**1**) biosynthetic gene cluster in *Penicillium paxilli*. Recombinant PaxD catalyzed a step-wise regular-type di-prenylation at the 21,22-positions of **1** with dimethylallyl diphosphate (DMAPP) as the prenyl donor. In this study, *atmD*, which is located in the aflatrem (**2**) biosynthetic gene cluster in *Aspergillus flavus* and encodes an enzyme with 32% amino acid identity to PaxD, was characterized using recombinant enzyme. When **1** and DMAPP were used as substrates, two major products and a trace of minor product were formed. The structures of the two major products were determined to be reversely mono-prenylated **1** at either the 20- or 21-position. Because **2** and β-aflatrem (**3**), both of which are **1**-related compounds produced by *A. flavus*, have the same prenyl moiety at the 20- and 21-position, respectively, AtmD should catalyze the prenylation in **2** and **3** biosynthesis. More importantly and surprisingly, AtmD accepted paspaline (**4**), which is an intermediate of **1** biosynthesis that has a similar structure to **1**, and catalyzed a regular mono-prenylation of **4** at either the 21- or 22-position, though the reverse prenylation was observed with **1**. This suggests that fungal indole diterpene prenyltransferases have the potential to alter their position and regular/reverse specificities for prenylation and could be applicable for synthesis of industrially useful compounds.

Introduction

The isoprenoid compounds found in nature, with over 50,000 known examples, include industrially useful compounds such as flavors, antibiotics, and plant hormones, among others (1–3). In some cases, isoprenoids are attached to other moieties, such as polyketide (4), indole/tryptophan (5), (iso)flavonoid (6), and phenazine moieties (7, 8). The isoprenoid moieties of these compounds are known to be important for their biological activities (9–11). For example, the presence of isoprenoid chains of varying lengths and types is a major determinant of the bioactivity of prenylated flavonoids (12–14). The polyketide-isoprenoid hybrid compounds furaquinocin, naphterpin, marinone, and napyradiomycin have been reported to have antitumor (15), antioxidative (16), and anticancer activities (17), and act as a non-steroidal estrogen-receptor antagonist (18), respectively. These molecules have similar polyketide moieties derived from 1,3,6,8-tetrahydroxynaphthalene (THN), showing that prenyl moieties play important roles in providing a diversity of biological activities. Therefore, prenyltransferases catalyzing the prenylation of various substrates at specific positions are very useful.

Recently, we characterized *paxD* (19), which is located next to *paxQ* in the **1** biosynthetic gene cluster and has weak similarities to fungal prenyltransferase genes (20). Recombinant PaxD catalyzed the successive regular attachment of DMAPP to positions 21 and 22 of **1** to form **5** via a mono-prenylated **1** intermediate (Fig. 1). A Blast search showed that the most homologous enzyme to PaxD was the *atmD* product (32% amino acid identity) (19), which is located in the **2** biosynthetic gene cluster in *A. flavus*. However, **2** and **3**, which are **1**-related compounds, were reversely mono-prenylated at the 20- and 21-position (21), respectively (Fig.1). Therefore, we examined whether AtmD catalyzes the reverse prenylation to produce these compounds or regular di-prenylation like PaxD. During the study, more importantly and surprisingly, we found that AtmD and PaxD accepted **4**, an intermediate of **1**

biosynthesis that has a similar structure to **1**, and that both enzymes unexpectedly showed different position and regular/reverse specificities to those with **1**. These results suggested that fungal indole diterpene prenyltransferases could be applicable for synthesis of important compounds, including bioactive compounds.

Experimental Section

General

Sequence analysis of polymerase chain reaction (PCR) fragments was performed by the dideoxy chain termination method with an automatic DNA sequencer (Li-Cor, model 4000L, Lincoln, NE, USA). Cell disruption was performed with an Ultrasonic Disruptor (TOMY, UD-200, Tokyo, Japan). Analysis of the samples during protein purification was performed using sodium dodecyl sulfate polyacrylamide gel electrophoresis (SDS-PAGE) and the proteins were visualized by Coomassie brilliant blue staining. Protein concentration was determined by the Bradford method (22) with bovine serum albumin as a standard. Plasmids from *E. coli* were prepared using a Qiagen plasmid kit (Hilden, Germany). All restriction enzymes, T4 ligase, and calf intestinal alkaline phosphatase were obtained from Toyobo (Osaka, Japan), and used according to the manufacturer's instructions. Farnesyl indole (**12**) and geranylgeranyl indole (**11**) were synthesized according to previously reported methods (23).

Strain

A. flavus NBRC 4295 was obtained from the Biological Resource Center, National Institute of Technology and Evaluation (NITE), Tokyo, Japan. This was used for the preparation of

atmD cDNA because we could not obtain *A. flavus* NRRL6541, from which the **2** biosynthetic gene cluster was isolated by Scott et al. The strain NBRC 4295 was suggested to produce **2** by LC-ESI-MS analysis. The presence of the **2** biosynthetic gene cluster in the genome was confirmed by PCR with specific primers (Table S1, Fig. S1), which were designed based on the sequences of each *atm* gene in *A. flavus* NRRL6541. Cultivation and cDNA preparation were performed using the same method we used for *P. paxilli* (19).

Cloning, overexpression, and purification of AtmD

The cDNA carrying the *atmD* gene was amplified by PCR using gene-specific primers: 5′-TTGCATGCATGTCCACTCCCAAGTCGGATACATGC-3′ and 5′-ATCTGCAGCTACTTGGAAAGCCCCTTCACATCTGAC-3′. After subcloning and sequence confirmation, a 1.3-kb fragment obtained by *Sph*I and *Pst*I digestion was ligated into the same sites of the pQE30 (Qiagen) to construct pQE30-AtmD. *E. coli* M15 carrying pQE30 (a control) and pQE30-AtmD were separately grown in L-broth supplemented with 100 μg/mL ampicillin. Expression and purification procedures were the same as previously reported (19, 24). For molecular mass and subunit structure determination of AtmD, the purified enzyme was loaded onto a HiLoad 26/60 Superdex 75 pg gel-filtration column (Amersham Biosciences, Piscataway, NJ, USA) and eluted with a buffer containing 50 mM Tris-HCl (pH 8.0) and 10 mM NaCl. The retention time of eluted AtmD was compared with those of marker proteins. The markers applied to the column were aldolase (158 kDa), albumin (67 kDa), ovalbumin (43 kDa), and chymotrypsinogen A (25 kDa) (GE Healthcare, Little Chalfont, UK).

In vitro assay of prenyltransferases

The standard assay mixture for AtmD and PaxD contained, in a final volume of 100 μL, 0.25 mM of prenyl acceptors, 0.5 mM of DMAPP, 50 mM Tris–HCl (pH 8.0), and 10 μM of enzyme. This mixture was incubated at 30°C overnight and the reaction was stopped by the addition of 100 μL methanol. The products were analyzed and purified by HPLC. The analytical conditions for the charts shown in Fig. 3A, 3B, 4A, 4B, 5A, and 5B were as follows: column, Merck Mightysil RP-18GP Aqua column (250 × 4.6 mm); mobile phase, acetonitrile in water (0 to 25 min, 70% acetonitrile; 25 to 40 min, 70 to 100%; 40 to 50 min, 100%); flow rate, 1.0 mL/min; detection, 230 nm. In Fig. S4A, S5A and S13, the conditions were: column, Merck Mightysil RP-18GP Aqua column (250 × 4.6 mm); mobile phase, acetonitrile in water (0 to 35 min, 0 to 100%; 35 to 60 min, 100%); flow rate, 1.0 mL/min; detection, 278 nm. The analytical conditions for the Waters XBridge^{TM} Phenyl 5 μm column (250 × 4.6 mm) (Fig. S6) were as follows: mobile phase, 65% (v/v) acetonitrile solution in water by isocratic flow; flow rate, 1.0 mL/min; detection, 230 nm.

The following compounds were used for examination of substrate specificity: **4** (purified from culture broth of *Aspergillus oryzae* carrying *paxG*, *paxM*, *paxB*, and *paxC*), cyclodipeptides (cyclo-L-Trp-L-Tyr, cyclo-L-Pro-L-Tyr, cyclo-L-His-L-Phe, cyclo-L-Phe-L-Pro, cyclo-L-Phe-L-Trp, cyclo-L-Phe-L-Leu, all of which were kindly provided by Dr. H. Kanzaki of Okayama University, Japan), hydroxynaphthalenes (1-naphthol, 1,3-dihydroxynaphthalene, 2,6-dihydroxynaphthalene, 2,7-dihydroxynaphthalene, 3,7-dihydroxy-2-naphtholic acid), indole, L-tryptophan and L-tyrosine.

The steady-state kinetic parameters of AtmD and PaxD were determined by fitting to the Michaelis-Menten equation. The assay was linear with respect to protein concentration up to 5 μg for 20 min incubation and no substrate inhibition was observed with **1**, **4**, or DMAPP up to 1.0 mM of each substrate. The assays for determination of the kinetic parameters of AtmD with **1** as a substrate contained, in a final volume of 100 μL, 50 mM Tris–HCl (pH 8.0), 0.5 mM DMAPP, 0.5 μg of enzyme, and 0.5 μM to 0.1 mM of **1**. When the concentration of **1** was fixed at 0.25 mM, the concentration of DMAPP was varied from 0.02 μM to 10 μM. The mixtures were incubated at 30°C for 10 min. For determination of the kinetic parameters with **4**, 0.01 mM to 1 mM of **4** with 0.5 mM DMAPP and 0.01 mM to 1.5 mM DMAPP with 0.25 mM of **4** were used as substrates. The mixtures were incubated at 30°C for 20 min.

Metal dependency of AtmD

Divalent metal ions (5 mM of Mg^{2+}, Ca^{2+}, Fe^{2+}, Cu^{2+}, Zn^{2+}, Mn^{2+}, Ni^{2+}, and Co^{2+}), or 5 mM ethylenediamine-*N*,*N*,*N'*,*N'*-tetra acetic acid (EDTA) were added to the standard reaction mixture.

Liquid chromatography–electrospray ionization mass spectrometry (LC/ESI-MS) analysis

Products formed in the *in vitro* assays were analyzed by LC/ESI-MS (Waters ACQUITY UPLC equipped with a SQD2) with a Waters ACQUITY UPLC BEH C18 1.7 μm column (2.1 × 50 mm) (Fig. 3C) or a Waters ACQUITY UPLC BEH Phenyl 1.7 μm column (2.1 × 50 mm) (Fig. 4C and 5C). The analytical conditions were as described previously (19).

Structural analysis of the reaction products formed from 1, 4, and 12 with DMAPP

The reaction products using **1, 4,** or **12** with DMAPP were fractionated with HPLC. ^{1}H- and

^{13}C-NMR spectra were recorded on a Bruker AMX-500 spectrometer: reversely mono-prenylated **1** at position 21 formed by AtmD (**6**), Fig. S14 to S20, HR-ESIMS: $[M+H]^+$ (calcd: 504.3108, observed: 504.3100); reversely mono-prenylated **1** at position 20 formed by AtmD (**7**), Fig. S14 and S21 to S26, HR-ESIMS: $[M+H]^+$ (calcd: 504.3108, observed: 504.3110); regularly mono-prenylated **4** at position 21 formed by AtmD and PaxD (**8**), Fig. S14 and S27 to S32, HR-ESIMS: $[M+H]^+$ (calcd: 490.3680, observed: 490.3675); regularly mono-prenylated **4** at position 22 formed by AtmD and PaxD (**9**), Fig. S14 and S33 to S38, HR-ESIMS: $[M+H]^+$ (calcd: 490.3680, observed: 490.3703); regularly mono-prenylated **12** at either the 5- (**13**) or 6-position (**14**) formed by AtmD, Fig. S14 and S39 to S44, HR-ESIMS: $[M+H]^+$ (calcd: 390.3155, observed: 390.3121). Key signals of indole and the dimethylallyl chain of **13** and **14** were assigned as follows: NMR δH ($CDCl_3$, 500 MHz) (Fig. S39) 1.60 (s), 1.68 (s), 1.75 (s), 1.76 (s), 1.90–2.20 (m), 3.44 (m, H1" and H1'), 5.09 (m), 5.12 (m), 5.38 (m), 5.43 (m), 6.86 (brs, 1H, H2-**14**), 6.89 (brs, 1H, H2-**13**), 6.94 (brd, *J* = 8.1 Hz, 1H, H5-**14**), 7.00 (brd, *J* = 8.2 Hz, 1H, H6-**13**), 7.13 (s, 1H, H7-**14**), 7.24 (d, *J* = 8.2 Hz, 1H, H7-**13**), 7.36 (s, 1H, H4-**13**), 7.48 (d, *J* = 8.1 Hz, 1H, H4-**14**), 7.74 (s, 1H, NH-**14**), 7.77 (s, 1H, NH-**13**). NMR δC ($CDCl_3$, 125 MHz) (Fig. S40) 16.0, 16.1, 17.7, 17.8, 24.0, 24.1, 25.7, 25.8, 26.6, 26.7, 26.8, 34.5 (C1"-**13**), 34.6 (C1"-**14**), 39.7 (x2), 110.2 (C7-**14**), 110.8 (C7-**13**), 115.8 (C3-**13**), 116.0 (C3-**14**), 118.0 (C4-**13**), 118.9 (C4-**14**), 120.2 (C5-**14**), 120.6 (C2-**14**), 121.4 (C2-**13**), 122.8 (C6-**13**), 123.0 (x2), 124.1, 124.3, 124.4, 124.6, 125.7 (C3a-**14**), 127.8 (C3a-**13**), 131.3, 131.5, 131.9, 132.5 (C5-**13**), 135.0, 135.1 (C7a-**13**), 135.5 (x2), 135.8 (C6-**14**), 137.0 (C7a-**14**).

Results

Functional analysis of AtmD

A cDNA of *atmD* was amplified based on the nucleotide sequence of the cDNA reported by Scott et al. (21) (GenBank; CAP53937). The predicted gene product consisted of 435 amino acids (GenBank; AB778117) and had 96% amino acid identity with CAP53937 (Fig. S2). The AtmD cDNA was cloned into the pQE30 vector for protein expression in *E. coli*. His-tagged AtmD recombinant enzyme was successfully expressed as a soluble form. Purified enzymes were obtained by Ni^{2+} column chromatography and successive desalting with Amicon Ultra devices. The obtained recombinant AtmD with a calculated molecular mass of 46 kDa was subjected to gel filtration and SDS-PAGE analyses. As shown in Fig. 2, one major peak with a calculated molecular mass of 95 kDa and a band of approximately 46 kDa were detected by gel filtration and SDS-PAGE, respectively, suggesting that AtmD forms a homo-dimer similar to PaxD.

The recombinant AtmD was used for *in vitro* assay. We used commercially available **1** as a prenyl acceptor, which has a similar structure to paspalinine (**10**), a probable intrinsic substrate (Fig. 1). After the recombinant AtmD was incubated with **1** and DMAPP, the reaction products were analyzed by HPLC. Two major products and a trace of minor product (Fig. 3A) were specifically detected. Total ion chromatograms obtained by LC/ESI-MS analysis showed three specific peaks with molecular masses corresponding to mono-prenylated **1** (Fig. S3). Moreover, selected ion chromatograms and their mass spectra strongly suggested that all products were mono-prenylated **1** (Fig. 3C). Because the yield of the minor product was low, the exact structures of the two major products were analyzed. HR-ESIMS of both products indicated the molecular formula $C_{31}H_{41}NO_4$, supporting that both products were mono-prenylated **1**. The ^{1}H-NMR spectra of one major product (**6**)

showed new signals assigned to a reversely prenylated moiety at δ = 5.04 (dd, 1H), δ = 5.11 (dd, 1H), δ = 6.11 (dd, 1H), and 1.47 (s, 6H). Extensive NMR data analysis, including COSY, HSQC, HMBC, and NOESY, proved the structure was reversely mono-prenylated **1** at position 21 (**6**) (Table S3, and Fig. S15 to 20). The ^{1}H-NMR spectra of the other major product (**7**) also showed new signals for a reversely prenylated moiety at δ = 4.88 (d, 1H), δ = 5.00 (d, 1H), δ = 6.26 (dd, 4H), 1.52 (s, 3H), and 1.53 (s, 3H). Subsequently, extensive NMR data analysis, including COSY, HSQC, HMBC, and NOESY, proved the structure was reversely mono-prenylated **1** at position 20 (**7**) (Table S4, and Fig. S21 to 26). Considering that the *atmD* gene is involved in the **2** biosynthetic gene cluster and that **2** and **3** have a reversely attached prenyl moiety at the same positions as those formed with **1** (Fig. 1), AtmD should catalyze prenylation in **2** and **3** biosynthesis.

Biochemical characterization of AtmD

The substrate specificity of the AtmD enzyme was investigated. For the prenyl acceptor, compounds related to indole diterpene biosynthesis, such as tryptophan, indole, indole-3-glycerol phosphate, **4**, **11**, and **12** (Fig. 1) were examined with DMAPP as a prenyl donor. We also used several cyclo-dipeptides and hydroxynaphthalenes because they were reported to be utilized by many fungal prenyltransferases (25–29). Of these compounds, **4** (Fig. 4), **11** (Fig. S5) and **12** (Fig. S4) were suggested to be mono-prenylated by LC-ESI-MS analysis. Because the yield of prenylated **11** was low, the structures of the prenylated **4** and **12** were determined. HR-ESIMS of the former and latter products indicated the molecular formulas $C_{33}H_{47}NO_2$ and $C_{28}H_{39}N$, supporting the production of mono-prenylated **4** and **12**. The exact structures of both products were elucidated by NMR analysis but both samples were a mixture of two closely related compounds. We tried to separate each of the compounds using several different columns and the XBridge^{TM} Phenyl Column was found to be effective (Fig. S6). In the case of mono-prenylated **4**, the yield was relatively high and

each of the products was successfully separated and used for NMR analysis. Very interestingly and surprisingly, the ^{1}H-NMR spectra of **8** showed new signals for a regularly prenylated moiety at δ = 3.40 (d, 2H), δ = 5.38 (m, 1H), δ = 1.73 (s, 3H), δ = 1.75 (s, 3H) (Table S5 and Fig. S27 to S32). **9** also showed similar ^{1}H-NMR spectra with characteristic signals at δ = 3.41 (d, 2H), δ = 5.37 (m, 1H), δ = 1.73 (s, 3H), δ = 1.73 (s, 3H) (Table S6 and Fig. S33 to S38). Finally, one was determined to be regularly mono-prenylated **4** at the 21-position (**8**) and the other regularly mono-prenylated **4** at the 22-position (**9**). This was contrary to our expectations because reverse prenylation at the 20- and 21- positions (**7**, **6**) occurred with **1** (Fig. 3). For mono-prenylated **12**, we conducted NMR analysis without separation of the two regioisomers (1:2.6 mixture) because the low yield prevented us from isolating a sufficient amount of each product. Typical signals for a regular dimethylallyl moiety were found at δ = 3.44 (m, 2H) and δ = 5.38 (m, 1H). Key HMBC, H-H COSY, and NOESY correlations were similar to those of **8** and **9**, suggesting that the prenylation takes place at the 5- and 6-positions on the indole moiety (Fig. S39 to S44). Taking these results together, the products were determined to be regularly mono-prenylated **12** at the 5- and 6-positions (**13** and **14**).

We next examined the substrate specificity of the prenyl donors. Aside from DMAPP, geranyl diphosphate, farnesyl diphosphate, and geranylgeranyl diphosphate were examined. However, no products were formed with **1** and **4** as prenyl acceptors.

The biochemical properties of AtmD were investigated using **1** and DMAPP as substrates. Under the conditions described in the Experimental Section, product formation was optimal at 50°C and around pH 7.0 (Fig. S7 and S8, respectively). The enzyme showed similar activity regardless of the presence of 5 mM of EDTA, suggesting that it did not require Mg^{2+} for its activity. In contrast, Cu^{2+} and Zn^{2+} significantly inhibited its activity. (Fig. S9).

The kinetic parameters of AtmD were investigated. The enzyme reaction followed

Michaelis-Menten kinetics. Using Hanes-Woolf plots (Fig. S10), the *Km* values were calculated as 13.8 ± 0.9 μM for **1** and 2.3 ± 0.1 μM for DMAPP. The *k*cat values were calculated as 0.38 ± 0.01/sec. We also investigated the kinetic parameters with **4** as the substrate (Fig. S11). The *Km* values were calculated as 131 ± 5 μM and 302 ± 11 μM for **4** and DMAPP, respectively. The *k*cat value was 0.09 ± 0.001/sec and the *kcat*/*Km* value was considerably lower than for **1**. This low value was consistent with the fact that prenylated **4** has not been reported as a natural product.

PaxD also accepted 4

Because AtmD accepted **4**, **11**, and **12**, we examined whether PaxD, which was previously shown to catalyze step-wise regular di-prenylation at the 21,22-positions of **1** to form **5**, was also able to use these compounds as prenyl acceptors. In this case, **4** (Fig. 5) and **12** (Fig. S4) were suggested to be mono-prenylated by LC-ESI-MS analysis and no diprenylated products were detected. The retention times and the observed mass spectra of both products were the same as those of the products formed by AtmD with **4**. The products formed from **4** also contained two closely related compounds (Fig. S6) and each of the products was purified and determined to be the same ones (**8** and **9**) formed by AtmD from **4** and DMAPP. Then, the kinetic parameters of PaxD were compared with those of AtmD. PaxD showed a similar *Km* value for **4** (124 ± 8 μM) and a very low value for DMAPP (7.9 ± 0.4 μM). The *k*cat value (0.07/sec) was almost the same as that of AtmD (Fig. S12).

Discussion

In this study, we showed that AtmD and PaxD could accept the intermediate compounds of **1** biosynthesis. AtmD, whose intrinsic substrate is **10**, utilized **1**, **4**, **11**, and **12**. PaxD also accepted **4** and **12** besides its real substrate **1**. These results suggested that prenyltransferases responsible for indole diterpene biosynthesis possess broad substrate

specificities. To examine this possibility, we investigated the substrate specificity of PaxC, which has been shown to catalyze the formation of geranylgeranyl indole from geranylgeranyl diphosphate and indole-3-glycerol phosphate (or indole) (30) and has no similarities to PaxD or AtmD. Although PaxC accepted none of the compounds used as prenyl acceptors for the same assay with AtmD and PaxD, the enzyme accepted farnesyl diphosphate as a prenyl donor to yield **12** (Fig. S13) with a slightly lower *kcat*/*Km* value (16.6 s^{-1} mM^{-1}, Table S2) than for GGDP (278.1 s^{-1} mM^{-1}) (30).

More importantly and surprisingly, AtmD catalyzed prenylation of **1** and **4** at different positions and with regular/reverse specificities. AtmD catalyzed a reverse mono-prenylation either at position 20 (**7**) or 21 (**6**) with **1** and DMAPP as substrates (Fig. 3). In contrast, regular mono prenylation either at position 21 or 22 (**8, 9**) was observed with **4** as a substrate (Fig. 4). Moreover, PaxD, which had been shown to produce a regularly di-prenylated product at the 21,22-positions (**5**) from **1** (19), catalyzed the same reactions as those of AtmD with **4** (Fig. 5). We are unable to estimate the reaction mechanisms to explain why these enzymes altered their position specificity, the regular/reverse mode for prenylation, and the number of introduced DMAPP to structurally related compounds; additional experiments such as molecular evolution engineering and site-directed mutagenesis based on x-ray structures of the enzymes may give us an answer.

Besides the enzymes we studied, CdpNPT (31), AnaPT (32), and CdpC3PT (33), whose real substrates are probably cyclo-L-Trp-L-Tyr, (*R*)-benzodiazepinedione, and several cyclic dipeptides, respectively, were recently shown to accept hydroxynaphthalenes as substrates (28). FtmPT1 was also demonstrated to catalyze the prenylation of a nonaromatic carbon of an indole derivative to give α-prenylindolylbutenone (34). Considering these previous results and our current study together, some fungal prenyltransferases are suggested to have the potential to accept a variety of substrates with broad position and regular/reverse mode

specificities. Such enzymes could therefore be applicable for synthesis of industrially useful compounds.

Moreover, many cyclic dipeptide prenyltransferases have been reported to accept cyclic dipeptide/amino acid derivatives different from their intrinsic substrates (35, 36, 38-41). For example, FgaPT2, FtmPT1, 7-DMATS have strict position specificities and essentially introduce DMAPP into the same positions as their intrinsic substrates (C4-, C2-, and C7-positions of the indole moiety, respectively). SirD also selectively introduces DMAPP into the C4-benzene ring. Therefore, these enzymes could be applicable for position-specific prenylation.

Acknowledgments This work was supported by the Grants-in-Aid for Scientific Research (23108101 to T. Dairi and 22108002 to H. Oikawa) from the Japan Society for the Promotion of Science (JSPS).

References

1. **Christianson DW.** 2007. Chemistry. Roots of biosynthetic diversity. Science **316:**60-61.

2. **Connolly JD, Hill RA.** 1992. Dictionary of terpenoids. New York: Chapman and Hall.

3. **Dewick PM.** 2002. The biosynthesis of C5-C25 terpenoid compounds. Nat. Prod. Rep. **19:**181-222.

4. **Lo HC, Entwistle R, Guo CJ, Ahuja M, Szewczyk E, Hung JH, Chiang YM, Oakley BR, Wang CC.** 2012. Two separate gene clusters encode the biosynthetic

pathway for the meroterpenoids austinol and dehydroaustinol in *Aspergillus nidulans*. J. Am. Chem. Soc. **134:**4709-4720.

5. **Steffan N, Grundmann A, Yin WB, Kremer A, Li SM.** 2009. Indole prenyltransferases from fungi: a new enzyme group with high potential for the production of prenylated indole derivatives. Curr. Med. Chem. **16:**218-231.

6. **Tahara S, Ibrahim RK.** 1995. Prenylated Isoflavonoids - an Update. Phytochemistry **38:**1073-1094.

7. **Izumikawa M, Khan ST, Takagi M, Shin-ya K.** 2010. Sponge-derived *Streptomyces* producing isoprenoids via the mevalonate pathway. J. Nat. Prod. **73:**208-212.

8. **Saleh O, Haagen Y, Seeger K, Heide L.** 2009. Prenyl transfer to aromatic substrates in the biosynthesis of aminocoumarins, meroterpenoids and phenazines: the ABBA prenyltransferase family. Phytochemistry **70:**1728-1738.

9. **Dalziel JE, Finch SC, Dunlop J.** 2005. The fungal neurotoxin lolitrem B inhibits the function of human large conductance calcium-activated potassium channels. Toxicol. Lett. **155:**421-426.

10. **Gonzalez MC, Lull C, Moya P, Ayala I, Primo J, Primo Yufera E.** 2003. Insecticidal activity of penitrems, including penitrem G, a new member of the family isolated from *Penicillium crustosum*. J. Agric. Food Chem. **51:**2156-2160.

11. **Singh SB, Ondeyka JG, Jayasuriya H, Zink DL, Ha SN, Dahl-Roshak A, Greene J, Kim JA, Smith MM, Shoop W, Tkacz JS.** 2004. Nodulisporic acids D-F: structure, biological activities, and biogenetic relationships. J. Nat. Prod.

67:1496-1506.

12. **Wang BH, Ternai B, Polya G.** 1997. Specific inhibition of cyclic AMP-dependent protein kinase by warangalone and robustic acid. Phytochemistry **44:**787-796.

13. **Maitrejean M, Comte G, Barron D, El Kirat K, Conseil G, Di Pietro A.** 2000. The flavanolignan silybin and its hemisynthetic derivatives, a novel series of potential modulators of P-glycoprotein. Bioorg. Med. Chem. Lett. **10:**157-160.

14. **Murakami A, Gao G, Omura M, Yano M, Ito C, Furukawa H, Takahashi D, Koshimizu K, Ohigashi H.** 2000. 1,1-Dimethylallylcoumarins potently suppress both lipopolysaccharide- and interferon-gamma-induced nitric oxide generation in mouse macrophage RAW 264.7 cells. Bioorg. Med. Chem. Lett. **10:**59-62.

15. **Komiyama K, Funayama S, Anraku Y, Ishibashi M, Takahashi Y, Omura S.** 1990. Novel antibiotics, furaquinocins A and B. Taxonomy, fermentation, isolation and physico-chemical and biological characteristics. J. Antibiot. **43:**247-252.

16. **Shin-ya K, Imai S, Furihata K, Hayakawa Y, Kato Y, Vanduyne GD, Clardy J, Seto H.** 1990. Isolation and structural elucidation of an antioxidative agent, naphterpin. J. Antibiot. **43:**444-447.

17. **Pathirana C, Jensen PR, Fenical W.** 1992. Marinone and debromomarinone: Antibiotic sesquiterpenoid naphthoquinones of a new structure class from a marine bacterium. Tetrahedron Lett. **33:**7663-7666.

18. **Shiomi K, Nakamura H, Iinuma H, Naganawa H, Isshiki K, Takeuchi T, Umezawa H, Iitaka Y.** 1986. Structures of new antibiotics napyradiomycins. J.

Antibiot. **39:**494-501.

19. **Liu C, Noike M, Minami A, Oikawa H, Dairi T.** 2013. Functional analysis of a prenyltransferase gene (*paxD*) in the paxilline biosynthetic gene cluster. Appl. Microbiol. Biotechnol. doi; 10.1007/s00253-013-4834-9.

20. **Young C, McMillan L, Telfer E, Scott B.** 2001. Molecular cloning and genetic analysis of an indole-diterpene gene cluster from *Penicillium paxilli*. Mol. Microbiol. **39:**754-764.

21. **Nicholson MJ, Koulman A, Monahan BJ, Pritchard BL, Payne GA, Scott B.** 2009. Identification of two aflatrem biosynthesis gene loci in *Aspergillus flavus* and metabolic engineering of *Penicillium paxilli* to elucidate their function. Appl. Environ. Microbiol. **75:**7469-7481.

22. **Bradford MM.** 1976. A rapid and sensitive method for the quantitation of microgram quantities of protein utilizing the principle of protein-dye binding. Anal. Biochem. **72:**248-254.

23. **Zhu X, Ganesan A.** 2002. Regioselective synthesis of 3-alkylindoles mediated by zinc triflate. J. Org. Chem. **67:**2705-2708.

24. **Noike M, Liu C, Ono Y, Hamano Y, Toyomasu T, Sassa T, Kato N, Dairi T.** 2012. An enzyme catalyzing *O*-prenylation of the glucose moiety of fusicoccin A, a diterpene glucoside produced by the fungus *Phomopsis amygdali*. Chembiochem **13:**566-573.

25. **Grundmann A, Li SM.** 2005. Overproduction, purification and characterization of

FtmPT1, a brevianamide F prenyltransferase from *Aspergillus fumigatus*. Microbiology **151:**2199-2207.

26. **Haug-Schifferdecker E, Arican D, Bruckner R, Heide L.** 2010. A new group of aromatic prenyltransferases in fungi, catalyzing a 2,7-dihydroxynaphthalene 3-dimethylallyl-transferase reaction. J. Biol. Chem. **285:**16487-16494.

27. **Yin S, Yu X, Wang Q, Liu XQ, Li SM.** 2013. Identification of a brevianamide F reverse prenyltransferase BrePT from *Aspergillus versicolor* with a broad substrate specificity towards tryptophan-containing cyclic dipeptides. Appl. Microbiol. Biotechnol. **97:**1649-1660.

28. **Yu X, Xie X, Li SM.** 2011. Substrate promiscuity of secondary metabolite enzymes: prenylation of hydroxynaphthalenes by fungal indole prenyltransferases. Appl. Microbiol. Biotechnol. **92:**737-748.

29. **Zou HX, Xie XL, Linne U, Zheng XD, Li SM.** 2010. Simultaneous C7- and N1-prenylation of cyclo-L-Trp-L-Trp catalyzed by a prenyltransferase from *Aspergillus oryzae*. Org. Biomol. Chem. **8:**3037-3044.

30. **Tagami K, Liu C, Minami A, Noike M, Isaka T, Fueki S, Shichijo Y, Toshima H, Gomi K, Dairi T, Oikawa H.** 2013. Reconstitution of biosynthetic machinery for indole-diterpene paxilline in *Aspergillus oryzae*. J. Am. Chem. Soc. **135:**1260-1263.

31. **Yin WB, Ruan HL, Westrich L, Grundmann A, Li SM.** 2007. CdpNPT, an *N*-prenyltransferase from *Aspergillus fumigatus*: overproduction, purification and biochemical characterisation. Chembiochem **8:**1154-1161.

410 32. **Yin WB, Grundmann A, Cheng J, Li SM.** 2009. Acetylaszonalenin biosynthesis in
411 *Neosartorya fischeri*. Identification of the biosynthetic gene cluster by genomic
412 mining and functional proof of the genes by biochemical investigation. J. Biol. Chem.
413 **284:**100-109.
414 33. **Yin WB, Yu X, Xie XL, Li SM.** 2010. Preparation of pyrrolo[2,3-b]indoles carrying
415 a beta-configured reverse C3-dimethylallyl moiety by using a recombinant
416 prenyltransferase CdpC3PT. Org. Biomol. Chem. **8:**2430-2438.
417 34. **Chen J, Morita H, Wakimoto T, Mori T, Noguchi H, Abe I.** 2012. Prenylation of a
418 nonaromatic carbon of indolylbutenone by a fungal indole prenyltransferase. Org.
419 Lett. **14:**3080-3083.
420 35. **Unsold IA, Li SM.** 2005. Overproduction, purification and characterization of
421 FgaPT2, a dimethylallyltryptophan synthase from *Aspergillus fumigatus*.
422 Microbiology **151:**1499-1505.
423 36. **Steffan N, Unsold IA, Li SM.** 2007. Chemoenzymatic synthesis of prenylated indole
424 derivatives by using a 4-dimethylallyltryptophan synthase from *Aspergillus fumigatus*.
425 Chembiochem **8:**1298-1307.
426 37. **Wollinsky B, Ludwig L, Xie X, Li SM.** 2012. Breaking the regioselectivity of indole
427 prenyltransferases: identification of regular C3-prenylated
428 hexahydropyrrolo[2,3-b]indoles as side products of the regular C2-prenyltransferase
429 FtmPT1. Org. Biomol. Chem. **10:**9262-9270.
430 38. **Kremer A, Westrich L, Li SM.** 2007. A 7-dimethylallyltryptophan synthase from

Aspergillus fumigatus: overproduction, purification and biochemical characterization. Microbiology **153:**3409-3416.

39. **Kremer A, Li SM.** 2008. Potential of a 7-dimethylallyltryptophan synthase as a tool for production of prenylated indole derivatives. Appl. Microbiol. Biotechnol. **79:**951-961.

40. **Kremer A, Li SM.** 2010. A tyrosine *O*-prenyltransferase catalyses the first pathway-specific step in the biosynthesis of sirodesmin PL. Microbiology **156:**278-286.

41. **Zou HX, Xie X, Zheng XD, Li SM.** 2011. The tyrosine *O*-prenyltransferase SirD catalyzes *O*-, *N*-, and *C*-prenylations. Appl. Microbiol. Biotechnol. **89:**1443-1451.

Fig. 1 Summary of reactions catalyzed by AtmD and PaxD. The regular biosynthetic pathways are highlighted by bold arrows. Putative aflatrem and β-aflatrem biosynthetic pathways are also shown.

Fig. 2 Purified AtmD was analyzed by SDS-PAGE and gel filtration chromatography. (**A**) Molecular mass markers (lane 1) and purified AtmD (lane 2). (**B**) Elution profiles of the standard proteins [aldolase (a, 158 kDa), albumin (b, 67 kDa), ovalbumin (c, 43 kDa) and chymotrypsinogen A (d, 25 kDa); top] and purified AtmD (bottom, e).

Fig. 3 HPLC and LC/ESI-MS analysis of the reaction products formed from **1** and DMAPP by AtmD. The reaction products formed with (**A, C**) and without (**B**) AtmD were analyzed by HPLC (**A, B**) and LC/ESI-MS (**C–F**). Selected ion chromatograms (**C**) and spectra of the major products (**7** (**D**) and **6** (**E**)) and the minor product (**F**) indicated by the asterisk in **C** are shown.

Fig. 4 HPLC and LC/ESI-MS analysis of the reaction products formed from **4** and DMAPP by AtmD. The reaction products formed with (**A, C**) and without (**B**) AtmD were analyzed by HPLC (**A, B**) and LC/ESI-MS (**C–E**). Selected ion chromatograms (**C**) and spectra of **8** (**D**) and **9** (**E**) are shown. Asterisks indicate unknown products.

Fig. 5 HPLC and LC/ESI-MS analysis of the reaction products formed from **4** and DMAPP by PaxD. The reaction products formed with (**A, C**) and without (**B**) AtmD were analyzed by HPLC (**A, B**) and LC/ESI-MS (**C–E**). Selected ion chromatograms (**C**) and spectra of **8** (**D**) and **9** (**E**) are shown. The asterisk indicates an unknown product.

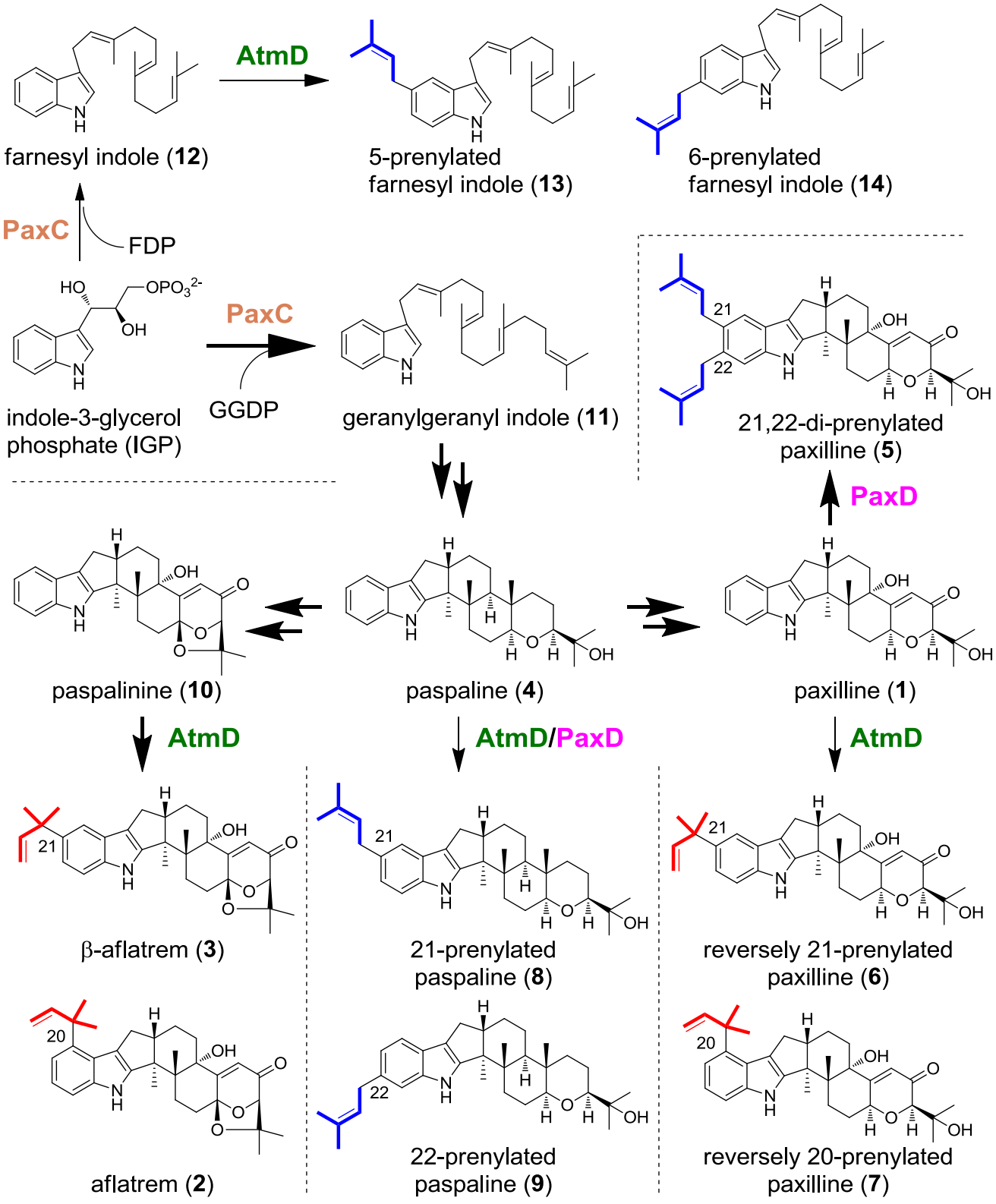
AtmD
farnesyl indole (12)
5-prenylated
farnesyl indole (13)
6-prenylated
farnesyl indole (14)
PaxC
FDP
HO
OPO3 2-
OH
indole-3-glycerol
phosphate (IGP)
PaxC
GGDP
geranylgeranyl indole (11)
21
22
21,22-di-prenylated
paxilline (5)
PaxD
paspalinine (10)
paspaline (4)
paxilline (1)
AtmD
AtmD/PaxD
AtmD
21
β-aflatrem (3)
21-prenylated
paspaline (8)
reversely 21-prenylated
paxilline (6)
20
aflatrem (2)
22
22-prenylated
paspaline (9)
20
reversely 20-prenylated
paxilline (7)

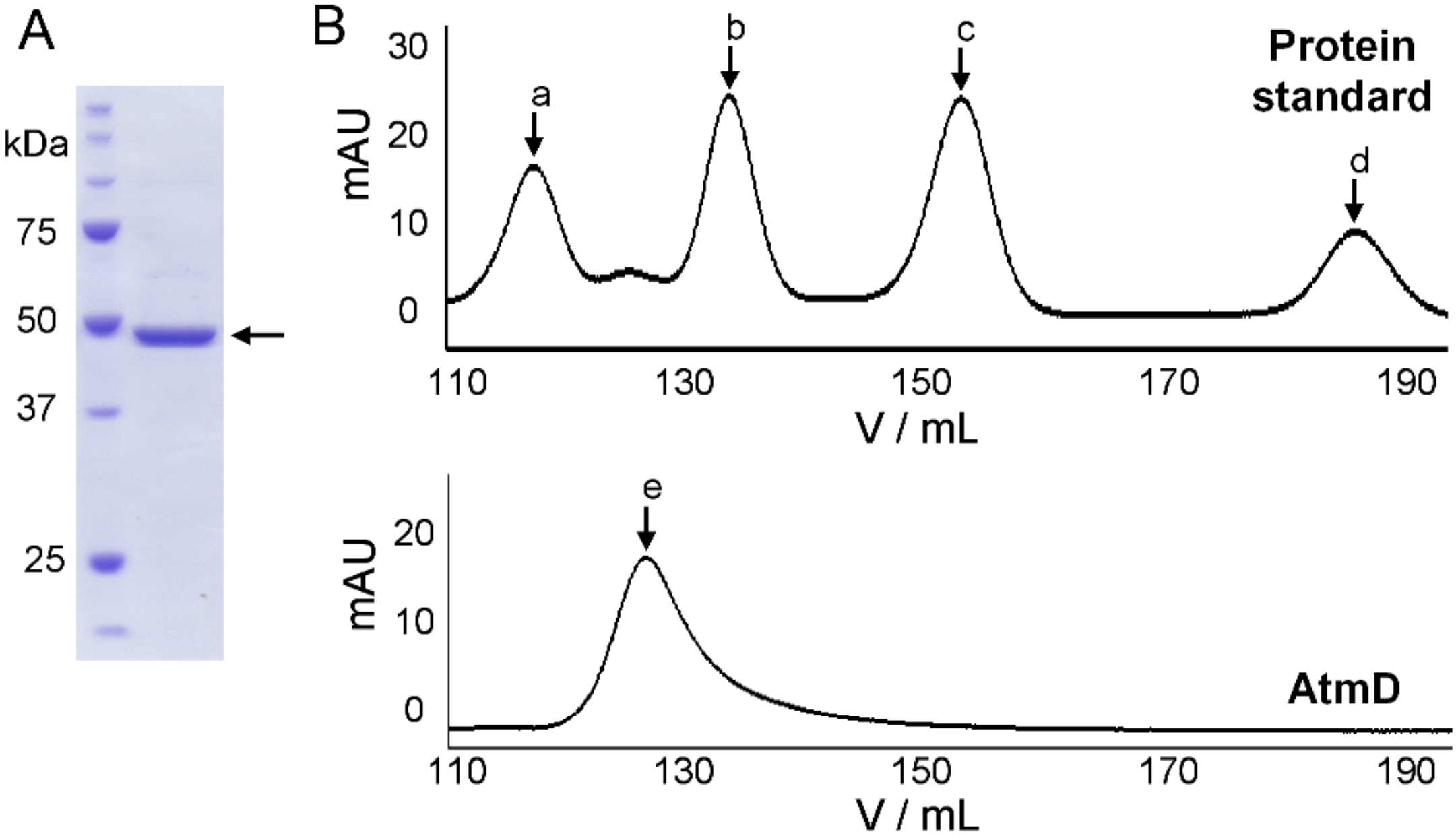
A
kDa
75
50
37
25
B
mAU
30
20
10
0
a
b
c
d
Protein standard
110
130
150
170
190
V / mL
mAU
20
10
0
e
AtmD
110
130
150
170
190
V / mL

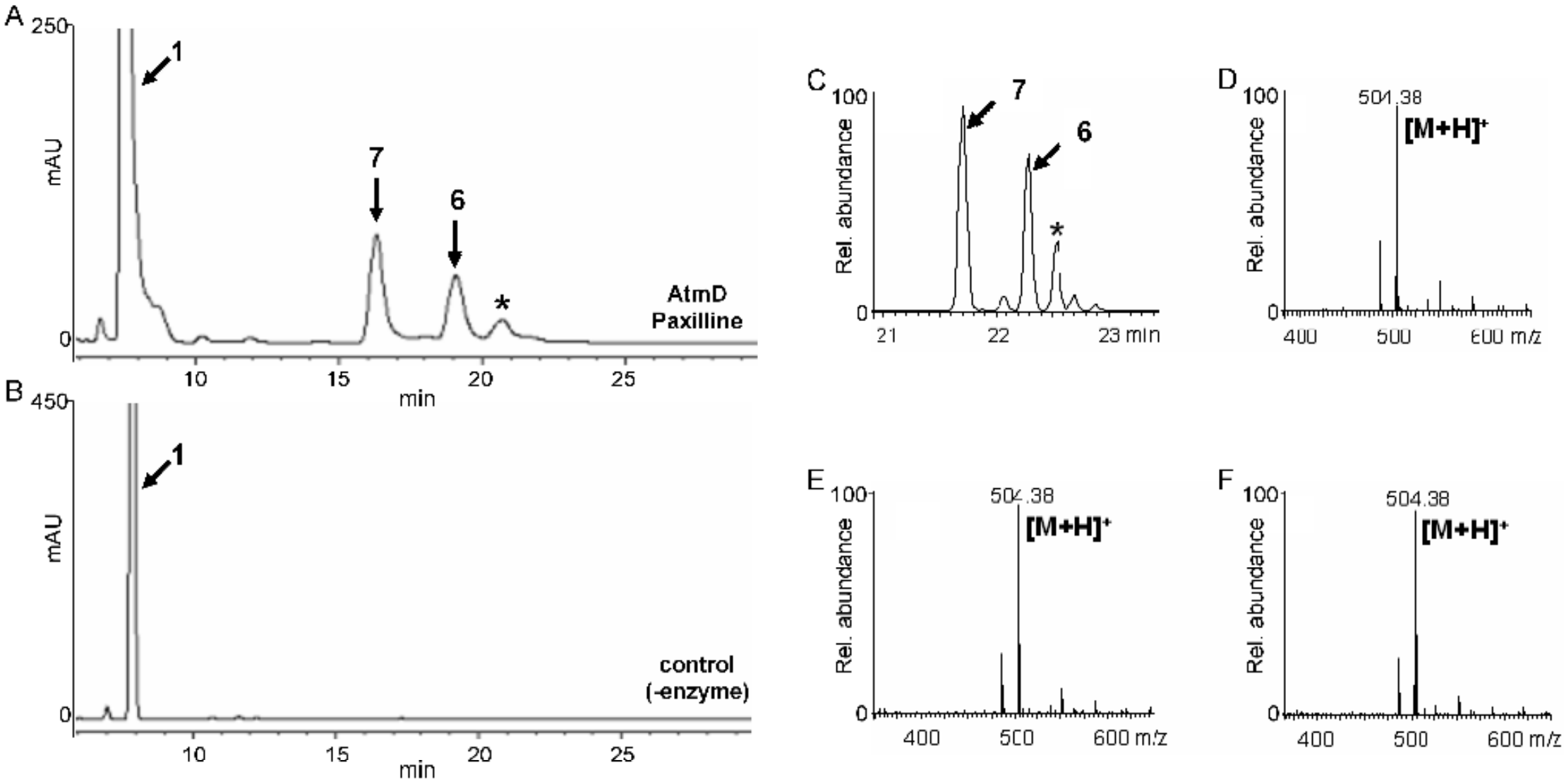
A
250
mAU
0
1
7
6
*
AtmD
Paxilline
10
15
20
25
min
B
450
mAU
0
1
control
(-enzyme)
10
15
20
25
min
C
100
Rel. abundance
0
7
6
*
21
22
23 min
D
100
Rel. abundance
0
504.38
[M+H]+
400
500
600 m/z
E
100
Rel. abundance
0
504.38
[M+H]+
400
500
600 m/z
F
100
Rel. abundance
0
504.38
[M+H]+
400
500
600 m/z

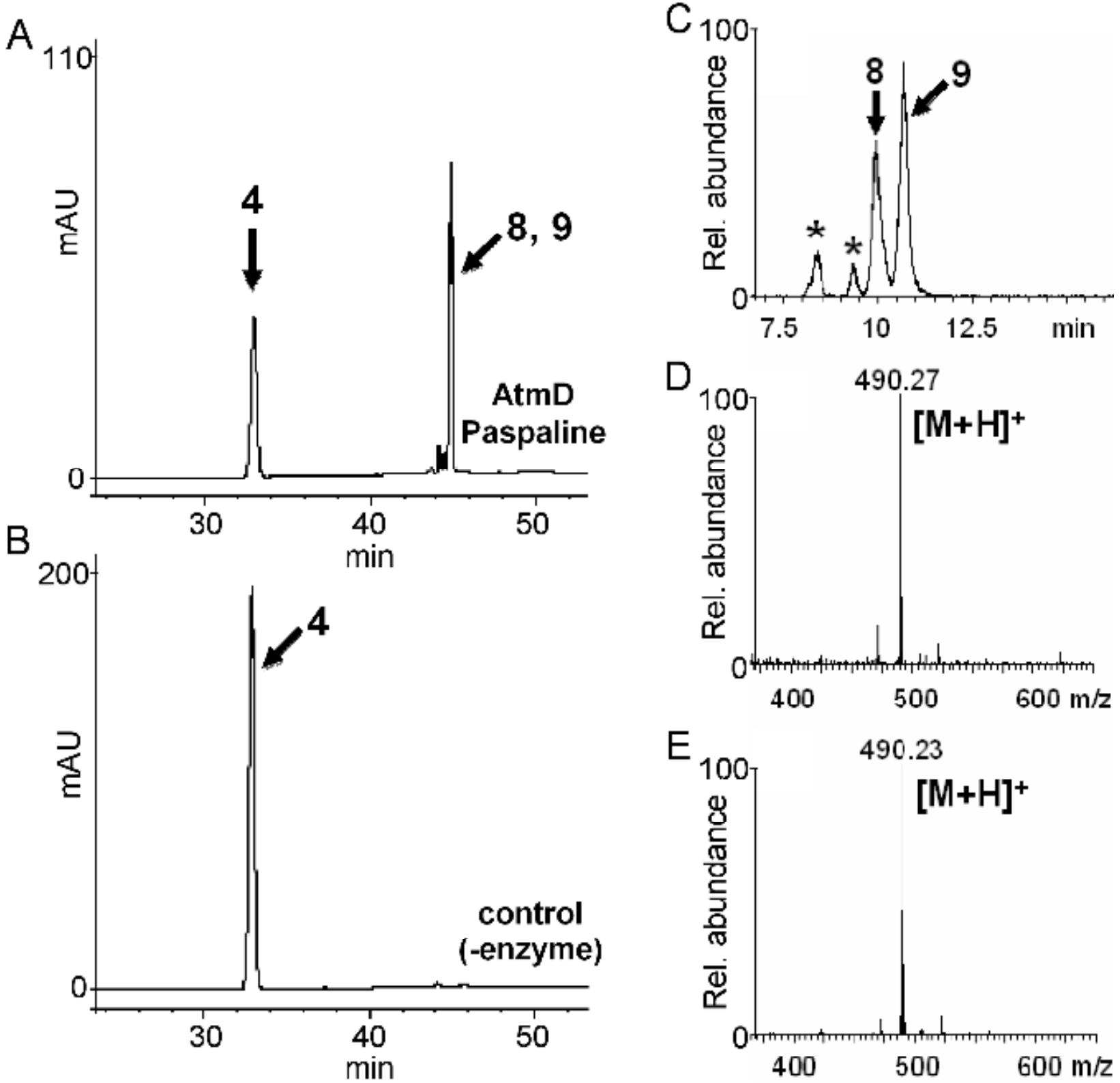
A
110
mAU
0
4
8, 9
AtmD
Paspaline
30
40
50
min
B
200
mAU
0
4
control
(-enzyme)
30
40
50
min
C
100
Rel. abundance
0
8
9
*
*
7.5
10
12.5
min
D
490.27
[M+H]+
100
Rel. abundance
0
400
500
600 m/z
E
490.23
[M+H]+
100
Rel. abundance
0
400
500
600 m/z

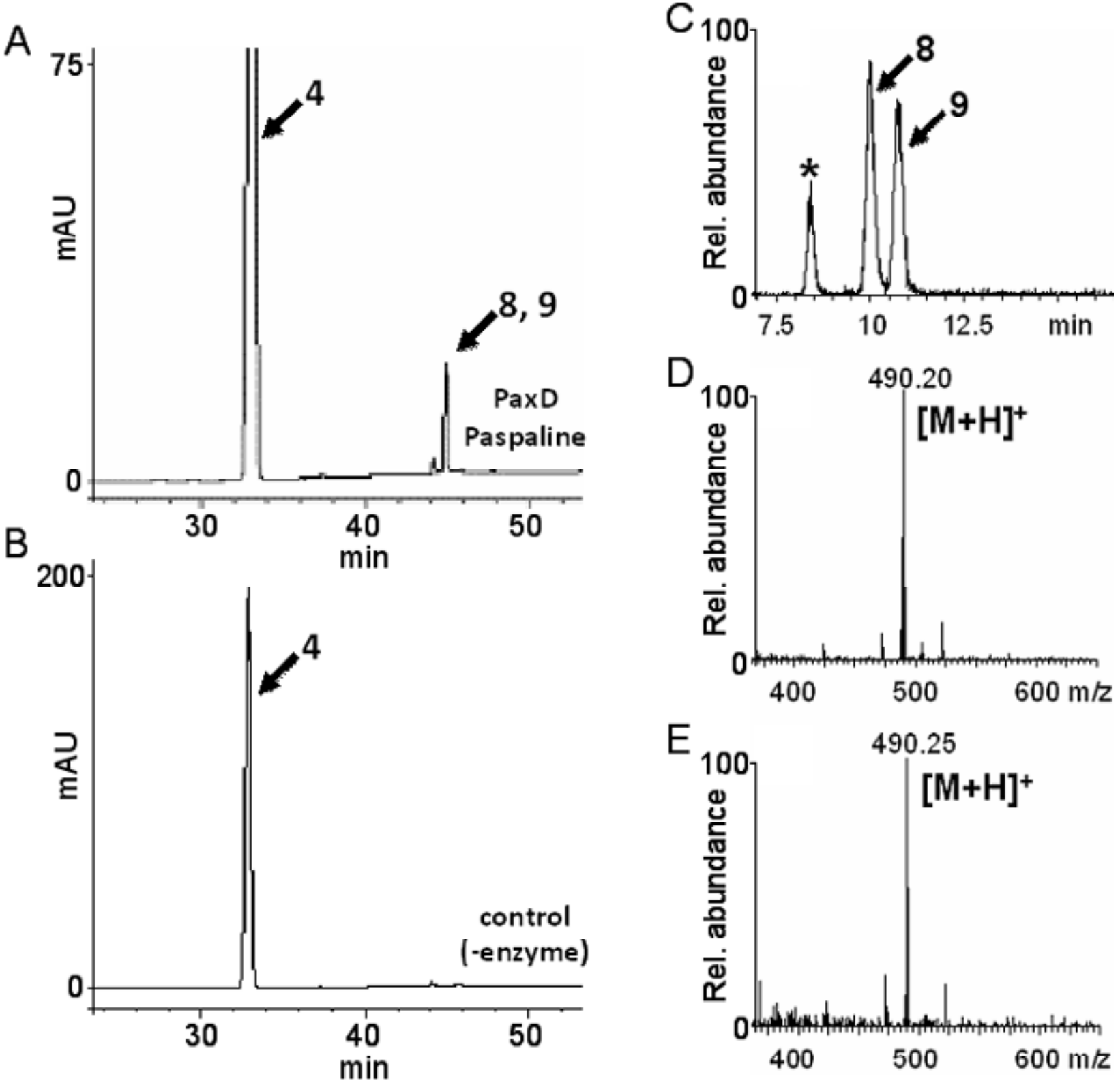
A
75
mAU
0
4
8, 9
PaxD
Paspaline
30
40
50
min
B
200
mAU
0
4
control
(-enzyme)
30
40
50
min
C
100
Rel. abundance
0
8
9
*
7.5
10
12.5
min
D
100
Rel. abundance
0
490.20
[M+H]+
400
500
600 m/z
E
100
Rel. abundance
0
490.25
[M+H]+
400
500
600 m/z